Full-waveform automatic location of small seismic events in an underground mine using synthetic strain Green's tensors

by S. Brijraj[1,2], S. Moolla[3], and R. Lynch[4]

Affiliation:
[1]University of KwaZulu Natal, Durban
[2]Institute of Mine Seismology, Stellenbosch
[3]Durban University of Technology, Durban
[4]Viotel Australia Pty Ltd, Australia

Correspondence to:
S. Brijraj

Email:
sahilbrijraj@gmail.com

Dates:
Received: 28 Oct. 2020
Revised: 28 Feb. 2022
Accepted: 10 Feb. 2024
Published: May 2024

How to cite:
Brijraj, S., Moolla, S., and Lynch, R. 2024. Full-waveform automatic location of small seismic events in an underground mine using synthetic strain Green's tensors. *Journal of the Southern African Institute of Mining and Metallurgy*, vol. 124, no. 5. pp. 269–278

DOI ID:
http://dx.doi.org/10.17159/2411-9717/1416/2024

ORCID:
S. Brijraj
http://orcid.org/0000-0002-0106-5709
S. Moolla
http://orcid.org/0009-0008-8045-4825
R. Lynch
http://orcid.org/0000-0002-7529-0669

Abstract

A reliable method to locate microseismic evets is an important objective for routine mine seismic monitoring. We developed an algorithm that can automatically and reliably locate an event from a single uniaxial trace. Signals created by microseismic events are recorded as seismograms that consist of direct P- and S-waves as well as the waves reflected off the underground excavations. We take advantage of the extra complexity these reflections introduce as they make the signal more unique. In our investigation we cross-correlated unaltered synthetic seismograms against trial waveforms created from a linear combination of appropriate waveforms from a library of numerically calculated strain Green's tensors. We use a single uniaxial synthetic seismogram to invert for the source location, six moment tensor components, and frequency. The resulting cost functions are constructed as maximal correlations at each node in the mine grid through the true source x-planes. This function is maximized by differential evolution to simultaneously yield the source parameters. Sensitivity tests such as shifting the mine plans and altering the background velocities of the media are investigated to test the robustness of the method. We contaminate the data with 40% white noise to test the resolution against simulated real recorded seismograms. The method is demonstrated using synthetic data calculated with a realistic underground 3D velocity model.

Keywords

mine seismicity, microseismic event, location, strain Green's tensor

Introduction

Microseismic monitoring is a standard technique routinely applied in more than 300 underground mines around the world (Mendecki and Young, 1993; Mendecki, 1997). Reliable location of microseismic events is vital in managing seismic hazard, and in understanding the rock mass response to mining. As more than 1 000 000 seismograms are recorded in underground mines each day, processing and locating techniques should be practical, quick, and – ideally – automatic.

Typically, arrays of seismic sensors are installed into short boreholes drilled from the underground tunnels. These sensors record both the direct body waves and the complex coda arising from multiple reflections and interactions with the tunnels and mining excavations. Routinely, the direct P- and S-wave arrivals are picked for a set of associated seismograms, and the seismic source is located using a variation of Geiger's method (Geiger, 1912). While 3D ray-tracing is sometimes used (Sewjee, Lynch, and du Toit, 2008), a homogeneous apparent velocity model is usually sufficiently accurate, and easier to maintain than a 3D velocity model of the changing mine. The nature of the velocity model is of paramount importance as its similarity to reality will determine how closely the synthetic and recorded waveforms match. If the wave velocities do not vary by more than a few per cent along the propagation path then the fixed velocity model holds well (Sewjee, Lynch, and du Toit, 2008). However, if there are localized regions of significant variation in wave velocities then the arrival times recorded may misrepresent the distance from the sensor to the hypocentre, which would reduce the reliability of the estimated hypocentre location. Voids within a mine represent areas with a high contrast in wave velocities to the surrounding rock. Lynch and Lotter (2007) estimated the variance of seismic wave velocities in cave mining at over 80%, while in open pit mines the variance between solid rock and air is over 90%.

There are three broad categories of event location calculation, distinguished by the nature of the velocity model being used. The first category assumes fixed-velocity models (Asch et al., 1996), based on the classic (Geiger, 1912) method. The second category comprises techniques that attempt to update the velocity model with information provided by recorded seismic events whose locations are yet to be calculated, while

simultaneously computing their hypocentres. (Thurber, 1986; Iyer and Hirahara, 1993). The third category is based on the location of seismic event hypocentres relative to each other, known as double differences in global seismology. (Waldhauser and Ellsworth, 2000; Waldhauser and Schaff, 2008). These methods employ the concept of using an already located earthquake, termed the master, as well as the associated slaves, which are earthquakes yet to be located relative to it.

Standard seismic location methods require identification of the P- and S-waves in recorded signals. This phase identification and the measurements of their arrival times are used to determine the event location. Phase picking is very difficult for signals with a relatively low signal-to-noise ratio. Techniques based on Kirchhoff migration utilize the entire waveform instead of phase identification. Signals from all sensors are superimposed and then maximized to identify the source location. Waveforms with a low signal-to-noise ratio as well as velocity models simulating very heterogeneous regions can make the results ambiguous (Gharti et al., 2010). Gajewski and Tessmer (2005) employed the backward extrapolation migration method to determine source location by considering the recorded waveforms as the boundary values for the reverse modelling. In other words. by reversing the waveforms in time and propagating them backwards through the model, the sensors can now be thought of as sources. The focus point then represents the event hypocentre. The origin time of the event is given by the time at which maximum focusing is observed. The spatial extent of the focus indicates the resolution power of the recorded waveform. Waveforms with a signal-to-noise ratio smaller than unity are difficult to manually process, as event arrivals are almost impossible to identify accurately. Gajewski and Tessmer showed that even such complex signals can be used to focus the event hypocentre very well.

Some methods require the use of envelopes and absolutes of the traces' amplitudes. These methods utilize the concept of delay and summing of the traces to enhance the signal-to-noise ratio (Ringdal and Kværna, 1989; Arnold, 1977; Gharti et al., 2010). This can be done by focusing on first arrivals, P-waves, or the most energetic parts of the signal, the S-waves. Siwei and Fomel (2013) used first arrivals to address the problem of working with a sparse source sampling by considering the derivative of travel time with respect to the source location. Kao and Shan (2004) proposed the source-scanning algorithm (SSA) to map the distribution of seismic sources in space and time. This method is limited, as instead of summing over the entire waveform it only sums absolute amplitudes at computed arrival times for predefined time windows around the most energetic portion of the trace. The problem with using envelopes of the waves is that information derived from the amplitude, phase, and position of the individual peaks is lost. This information is critical for learning about the moment tensor of the source. Thus in our study no envelopes are used. The full complex waveforms, comprising the direct body waves and the complex coda received later, are processed. The nature of all these peaks is intrinsically related to the mechanism of the event. We used a library of strain Green's tensors (SGTs) to create trial waveforms by linearly combining appropriate tensors. The scalars that are used to multiply and then combine the tensors representing the source mechanism, or moment tensor components. The trial waveforms are then cross-correlated against a synthetic data waveform. We employed the differential evolution (DE) code to optimize the full 10D problem and solve for the location, mechanism, and frequency.

Background theory

The theory behind this approach is quite simple. A library of SGTs is numerically calculated using a modified version of the finite difference code developed by Larsen and Schultz (1995b). The SGTs are derived from the Green's functions. The Green's functions are created using delta source-time functions, which are source impulses that contain all frequencies. The Green's functions fully describe the medium between the source and receiver as the waves sample every possible ray path between the two locations. Thus, a waveform produced at a source and recorded at a sensor should be reproducible by linearly combining Green's functions with the same trigger and recording locales. In our investigation, we focused on moment-tensor point sources. The moment tensor associated with an event, M_{ij}, is a 3 × 3 matrix, with equal off-diagonal elements, leaving six independent components. Thus, at every node in the model representing a potential source location, six SGT time functions must be created per sensor component (x, y, z). Seismograms, or displacement fields, generated as a result of moment-tensor sources are given by the general relationship (Aki and Richards, 2002)

$$u_n(x,t) = G_{ni,j}(x,t;\xi,0) * M_{ij}(t) \quad [1]$$

where the symbol (∗) denotes the convolution, u_n is the nth component of the displacement field (n = x, y, z), G the Green's function recorded at x for a unit force applied at ξ , and M the moment tensor. The moment tensor can be broken down into the multiplication of a scalar 3 × 3 matrix with a common source-time function, $s(t)$, thus $M_{ij}(t) = M_{ij} \times s(t)$. Summation convention applies to repeated indices. The index j after the comma (,) represents the partial derivative with respect to the source coordinates (ξ_j). Our approach uses the SGT, as demonstrated by Gharti et al. (2011). The spatial reciprocity of the Green's function means Equation [1] can be reformulated as

$$u_n(x,t) = E_{ij,n}(\xi,t;x,0) * M_{ij}(\xi,t) \quad [2]$$

where $E_{ij,n}$ is the SGT, which represents the strain components computed for a unit force applied in the *nth* direction. Due to the symmetry, the SGT has 18 independent components. It is related to the Green's functions by

$$E_{ij,n}(\xi,t;x,0) = \frac{1}{2}\left(G(\xi,t;x,0) + G_{jn,i}(\xi,t;x,0)\right) \quad [3]$$

The conversion of the Green's tensor to the SGT is far more appealing, as only three simulations are required for each individual source-sensor configuration, and not six, thereby reducing computational time as well as storage space for the library. Kawakatsu and Montagner (2008) showed that doing the time-reversal operation by reversing the received traces, $u_n(x, t)$, in time and convolving them with elements of the SGT library gave a good approximation of the source location by

$$M_{ij}(\xi,t) \approx E_{ij,n}(\xi,t;x,0) * u_n(x,t_0 - t) \quad [4]$$

where $u_n(x, t_0 - t)$ is the time-reversed version of the data $u_n(x, t)$. However, it is easier to use the traces as they are. The easier approach would be to simply cross-correlate the original received trace un (x, t) with either the Green's tensor or SGT libraries (Gharti et al., 2011) as

$$M_{ij}(\xi,t) \approx E_{ij,n}(\xi,t;x,0)Xu_n(x,t) \quad [5]$$

where the symbol *(X)* denotes the cross-correlation. Gharti et al. (2011) explain that this formulation of M_{ij} is not the actual moment tensor, but rather this quantity focuses at the correct source location and should give a qualitative estimation of the moment tensor. Using cross-correlation is preferred as it is computationally less expensive than convolution. In our study we take advantage of the reciprocity property of the SGTs and consider each location in the mine as a sensor, and each sensor as a source to reduce computational costs. The objective function at each location in the mine, ξ , and origin time t_0 is given as

$$S(\xi,t_0) = \left[M_{ij} \cdot E_{ij,n}(\xi,t;x,0) * s(t)\right]u_n(x,t) \quad [6]$$

For objective functions with multiple significant peaks we square the objective function values, which enhances any significantly high values as well as supressing lower insignificant peaks that may seem interesting but are actually regions of false positives. The region in our resulting cost function that reaches a maximum identifies the location of the source. The simulations are all triggered at time sample zero, thus origin time in this synthetic study was sample zero. This removed one degree of freedom from the problem. For purely synthetic, noiseless simulations a maximum correlation of unity is expected at the correct location. Where Gharti et al. (2011) could find a qualitative description of the source's moment tensor at the correct location, we inverted for the location, mechanism, and frequency simultaneously, thus fully describing the event all at once. We also used only a single uniaxial seismogram, whereas Gharti et al. (2011) used 18 triaxial traces. If this is successful it would be a great advantage in microseimic analysis.

Methodology

In this investigation we focused on running numerical synthetic simulations. The Pyhasalmi mine, located in central Finland (Figure 1), exploits a volcanogenic massive sulphide (VMS) deposit (Gharti et al., 2011). SGTs describe all possible paths between the sensor sites and every node in the model. The tensor elements also contain all possible frequencies as they are created using a unitary

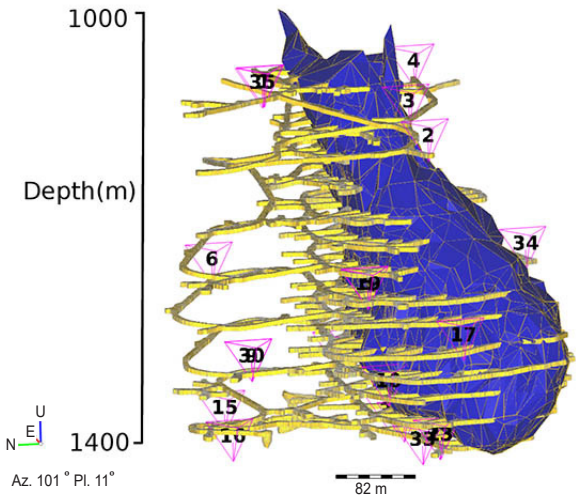

Figure 1—Pyhasalmi ore mine with surrounding infrastructure: the Copper/Zink ore body (dark blue), access tunnels (yellow) and seismic stations(numbered pyramids). (Gharti et al., 2011)

delta force source. Thus, in theory, any specific frequency wave for a specific path from a node in the model to a sensor should be retrieveable by linearly combining the appropriate tensor elements multiplied by unique independent scalars. All the simulations were carried out using a version of the 3D viscoelastic finite-difference code by Larsen and Schultz (1995a) modified by Dr H.N. Gharthi, which from here on will be referred to as E3d.

The SGT library is computed by solving the forward wave equation using a simple delta point source. The drawback to this method is that it requires physical storage space for the tensor element files, which contain a large amount of data. However, once the library is prepared any number of tests can be conducted on any number of specified regions of interest within the model. The library was constructed by taking advantage of the inherent reciprocity property of SGTs, which meant, computationally, we could consider the sensors as sources and each node in our mine plan as a sensor, thereby reducing the number of simulations required, as done by Gajewski and Tessmer (2005). However, unlike them we do not reverse our signals in time. Thus instead of using 250-squared scripts with one sensor per script for each of the three unitary forces *(F_x, F_y, F_z)*, it was more convenient to run scripts with one source and 250-squared sensors for each unitary force. Using this approach, each simulation took roughly just under 3 hours to complete a library on a single x-plane and roughly 2 Gb of RAM. The cost function is calculated at each grid point in the model using Equation [6]. Per location per sensor per component the six SGTs are linearly combined, then convolved with a source-time function of a specific frequency and shape to create a trial waveform, which is in turn correlated against the corresponding *n*th-component seismogram, *n* = .x, .y, .z.

For this paper a 250 Hz Ricker wavelet source-time function was used. The six scalars and frequency are optimized using DE to give the maximum value for the objective function at each node. If more than one sensor is considered then the total cost function at that location is the sum of each correlation between corresponding sensor-source traces. If the model and the mathematical operations are perfect. each sensor correlation should give the theoretically maximum value of unity at, and only at, the correct source location. If multiple sensors are considered then we just superimpose their correlations at each location and expect their contributions, given by (correlation per sensor)/(number of sensors), to yield a value of unity. We attempt to extend the work of Gharti et al. (2011) by reducing the number of traces used to just a single uniaxial trace.

Numerical results

We use a complex void-filled model. Voids are regions like tunnels, excavations, caves –essentially they are blocks of air within the model. Within these areas the P- and S-wave velocities drop to 0.3 km/s and zero, respectively. The Q-factor (attenuation) drops from 300 to 0.01. These effects will affect the arrival times of the P- and S-waves, as voids introduce reflections into the problem. The waves will reflect off the air/rock boundary and travel on a new ray path through the medium. This will result in different arrival times being recorded at the sensors and hence build the seismograms into a more complex waveform. These reflections do make the problem more complex, but also add an element of uniqueness. This is because waves that travel from one location will travel a very different path to a ray originating at a node right next to it, as it will strike different sections of voids at different angles, thus reflecting off in different paths. It is therefore expected that the cost function produced for inhomogeneous models will have a far

more unique maximum than the homogeneous case. We attempt to take full advantage of the highly complex coda as well as the direct body waves and use a single uniaxial seismogram to perform our inversion. Sensitivity tests are important to verify the robustness of any method. A major factor that affects the phase arrivals of events is the distribution of voids within the mine, such as tunnels, stopes, and shafts. Such areas cause reflections of seismic signals, which increase the complexity of the final received traces. The voids used here simulate the actual Pyhäsalmi mine plans. Another significant factor to consider is regions of variation in the velocity model. Such regions cause the phases to be received either later or earlier, depending on whether the r wave path is characterized by lower or higher velocities, respectively, than the expected background velocity of the host material, which is roughly 6 km/s for P-waves and 3.73 km/s for S-waves. The SGT library was constructed using a homogeneous velocity model with these velocities.

Figure 2 represents the resulting cost functions when the model has been altered to reflect realistically non-ideal situations. For our runs we simulate a source at node (x 180, y 105, z 105) in a 351-cubed node model. Since the model includes absorbing boundaries that are 50 nodes thick around our mine model, the physically feasible model is 250-cubed nodes. The model has a node spacing of 2 m. The x-, y-, and z-axes represent the extent in the north-south, east-west, and depth directions respectively. For the sensitivity tests we use a single uniaxial sensor located at node (x 169, y 117, z 55). The sensor is projected onto the true source x-plane, denoted by 'S ' at node (x 180, y 117, z 55) in Figure 2. Figure 2 shows the result of using the SGT library created using a single uniaxial sensor with a uniform background velocity model and a 250 Hz Ricker source, located at node (x 180, y 105, z 105), denoted by 'L', with a moment tensor [m_{xx} = 1.0, mxy = 0.5, m_{xz} = 0.2, m_{yy} = −1.0, $_{myz}$ = 0.1, m_{zz} = 0.1]. The calculated maximal source location is indicated by 'L'. The cost functions display the variation of maximal correlations per node through the x-plane of the true source (x-node = 180). Figure 2a shows the resulting cost function for a 250 Hz source correlated against the SGT library using a smoothly varying velocity model with randomly scattered regions of ±10% of the standard P-wave velocity of 6 km/s, as well as the tunnels and mine plans. Figure 2b displays the cost function for a source velocity model varying by ±20% of the maximum P-wave velocity in random scattered regions. These tests give an indication of the method's ability to incorporate changes in the background media that are not known and their effect on a definitive accurate location resolution. In both figures the correct location is retrieved, as well as an accurate approximation of the source mechanism.

Such tests are very important because in a real working mine there are regions characterized by higher or lower velocities than the standard assumed velocity for that particular mine. Any method that involves analysing waveforms produced in such media must either incorporate a model specified enough to portray the regions accurately, or more conveniently, be immune to such changes and thus, simply, assume a constant velocity background. Our tests show that we can assume a fixed velocity model.

Figure 2c shows the cost function for shifting the mine plans by 2 m in all three axial directions, resulting in a total shift of 3.5 m. Tests showed that an equally far shift in any direction yielded functionally identical results. This test is meant to represent errors in the surveying of the mine plans before they are digitized and used to create synthetic models. Since the problem of microseismic location is inherently due to the geometry of the ray paths and reflections off voids, an unknown shift in the mine plans could be detrimental to accurate results. However, unknown shifts of the plans of the order of a few metres did not affect the resolution of the resulting location. A powerful and promising outcome of these tests is that using a single uniaxial sensor produced almost perfect correlations (> 0.99) at the correct location.

Figure 3 shows the result of using a different sensor than in the tests displayed in Figure 2. Figure 3a shows the cost function through the x-plane of the true source location (x 180, y 105, z 105). The sensor is located at node (x 185, y 156, z 130), which is projected onto the true source x-plane at node (x 180, y 156, z 130). The sensor is centrally placed in the region of the cost function. There is a clear single, isolated narrow maximum peak at the correct location of (y 105, z 105) on this plane. The value rises to a correlation value of 0.99 at the correct location. This shows that a single uniaxial trace can be used to compare against an SGT library. Our results compare well to previous similar studies (Gharti et al., 2010, 2011). As can be seen from Figures 2 and 3a, the expected ring structure from using a single sensor is present. Figure 3a shows the circular distribution of elevated correlations around the sensor location; however, the maximum value along the perimeter is located only at the true source location. Figure 3b shows the comparison of the single uniaxial data trace (green) and the sum of the convolved SGTs (black) at the maximal location picked out by DE. DE gave final values of (y = 105, depth *(D)* = 105, *f* = 246 Hz, m_{xx} = 0.978, m_{xy} = 0.538, m_{xz} = 0.174, m_{yy} = −1.00, m_{yz} = 0.089, m_{zz} = 0.106), which are very close to the true source parameters.

To synthetically simulate a real seismogram, which is contaminated by noise composed of many frequencies, we added 40% white noise to the original 250 Hz data trace (see Figure 4). This was then used as our data, and as can be seen in Figure 4a the results are still very promising. In this case there is still a definitive peak in the cost function centred over the correct source location (y = 105, z = 105). Figure 4b shows the comparison of the contaminated data trace against the sum of the noiseless synthetic SGT waveforms. The high noise contamination is clearly dominant and reduces the correlation to 0.603;, however, it can clearly be seen the waveforms still follow the same low frequency vibration. DE gave final maximal values of [y = 105, *D* = 105, *f* = 244 Hz, m_{xx} = 1.0, m_{xy} = 0.43, m_{xz} = 0.15, m_{yy} = −0.79, m_{yz} = 0.06, m_{zz} = 0.143]. Again here, it can be seen that even with a very noisy signal the maximal parameters calculated come out very close to the true soure parameters, including the polarity of the moment tensor components and not just their magnitudes. To remove the some of the interference effect of the noise the signal was band-pass filtered between 20 and 480 Hz, as shown in Figure 4c. Final maximal parameters are [y = 105, *D* = 105, *f* = 252 Hz, m_{xx} = 0.86, m_{xy} = 0.42, mxz = 0.40, m_{yy} = −1.00, m_{yz} = 0.18, m_{zz} = −0.10). The correlation in this case increases to just over 0.98. This test has very important implications as it shows that we can still take a noisy signal, band-pass filter it around its central frequency, which is a parameter that is routinely retrieved, and then still use it in our method to give excellent results. The convenient aspect of this investigation is that once the SGT library has been constructed, we are able to simulate a source of any frequency, as well as, any combination of moment tensor components.

Application to a real event

The ultimate aim of this investigation is to retrieve the location of real recorded microseismic events in a working mine. Currently, IMS Trace software is used routinely as a tool to resolve an event's

location. Trace utilizes ray-tracing, and seismograms from at least three sensors are required to resolve the location of the event. Although this method works, quite often three waves are not recorded for an event. This means that all events that do not meet this threshold are ignored, which is a large waste of data. Thus, a method that can utilize only one or two sesimograms will be highly beneficial. Using a library of SGTs can solve this problem. Another factor to keep in mind is that most mines do not use many triaxial sensors, as uniaxial sensors are more cost-effective.

Thus, for a given event the data recorded may only be a single z-seismogram, as most uniaxial sensors are aligned along the z (depth) direction.

To test the method for real data an event recorded on 16 July 2015 in the Pyhäsalmi mine was utilized. The event was recorded on five sensors. We considered analysing a single sensor's trace. From Figure 6b it was found that sensor 16 had the highest correlation. The maximal frequency range was observed to be between 350 and 500 Hz . This seismogram, which was a single z-component

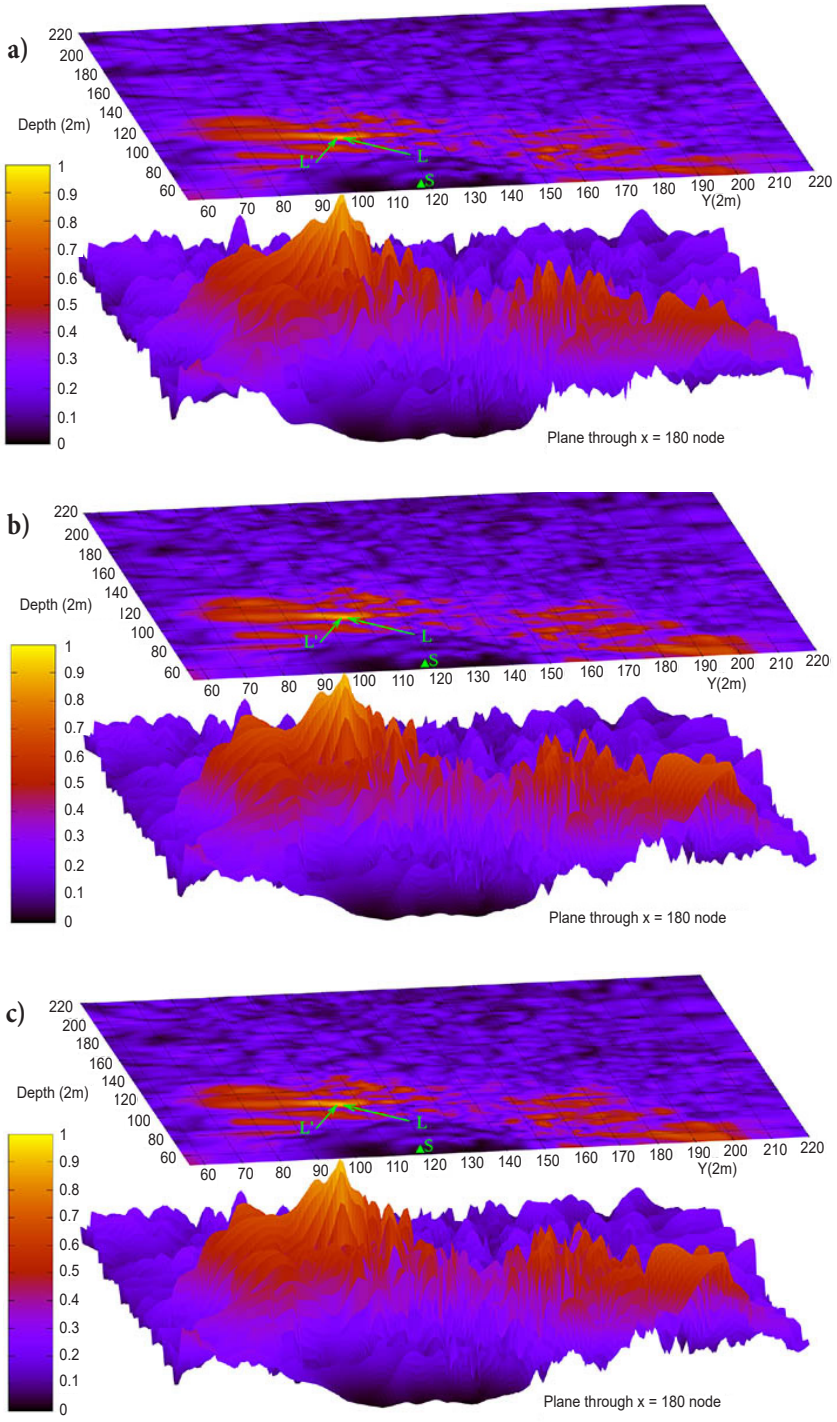

Figure 2— Sensitivity test objective functions for fixed-velocity strain Green's tensors library correlated against single uniaxial 250Hz noiseless data trace using a model with a) scattered regions of ±10% of the background velocity, V pmax , b) regions in a) increased to ±20% and c) mine-plans shifted by 2m in all three axial directions. True source, L, sensor, S, and calculated maximal location at L'. Maximal location matches true location exactly with correlations of 0.943, 0.93 and 0.937 respectively. General ring structure of elevated values is observed, and as expected near perfect zero values observed near the sensor

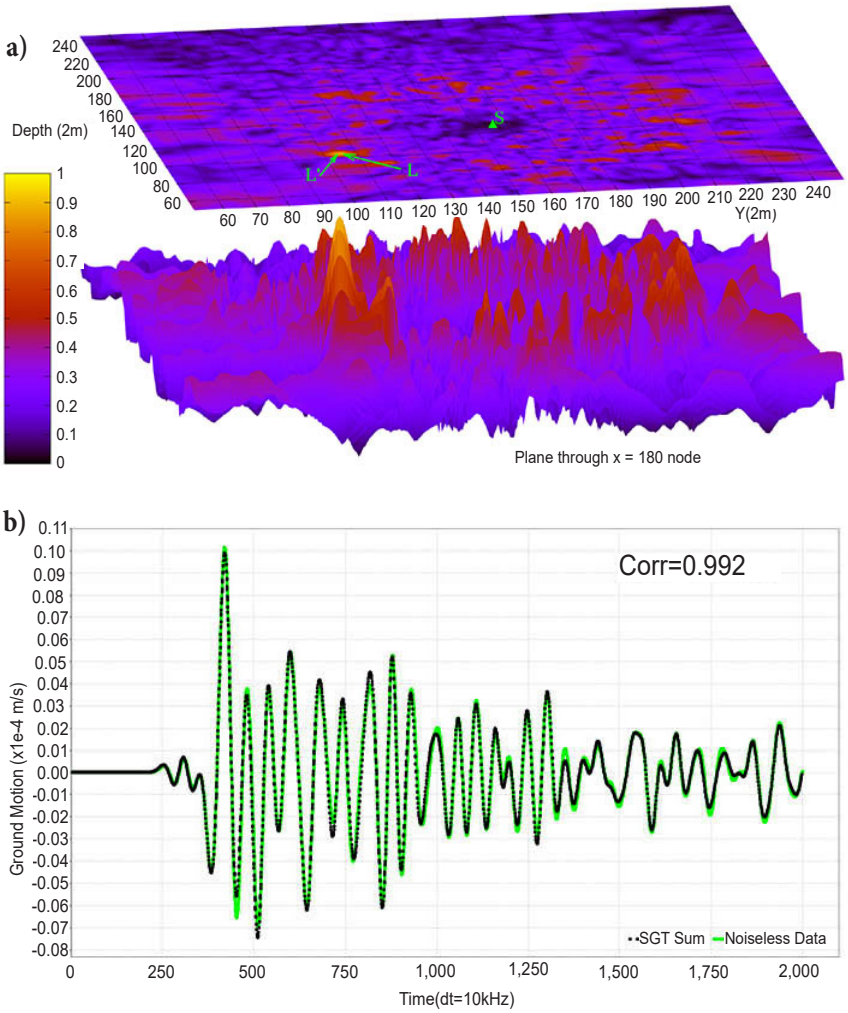

Figure 3— a)Objective function computed for noiseless 250Hz Ricker source. True source, L, sensor, S, and calculated maximal location at L'. Maximal location bright spot at node(y=105, Depth=105) matches real source at node(y=105, Depth=105) on this x-plane. Circular distribution of elevated values around sensor with radius of roughly 60m. The complex reflections in the signal help break up the ring and isolate a single pronounced peak at the correct location as a global maximum. As expected there are near-zero values near the sensor. b) Synthetic summed strain Green's tensors waveform(black) vs synthetic 250Hz data trace(green), with correlation of just over 0.991

seismogram, was correlated against a library of SGTs created using the contemporary mine model. The first aspect of this method would require some knowledge of the frequency as well as the temporal profile of the event trigger.

Tests pointed to using the Beresnev profile (Beresnev, 2001) for the source-time function in preference to the standard Ricker wavelet employed by E3d (Larsen and Schultz, 1995a) as best to match real recorded data. Using a Beresnev source-time function at a frequency of 375 Hz gave the best matching waveforms. This source-time function was used to convolve the SGT library and carry out the correlations. The preliminary results are displayed in the the cost functions seen in Figure 5. The location predicted by Trace was (x = 187, y = 123, z = 88). However, our method found the location at (187,132, 93). This is roughly a 20 m shift, considering a node spacing of 2 m. This could be explained by the fact that Trace assumes straight ray paths, essentially triangulation, which does not take into account the effect of the voids on arrival times. Our method inherently uses the effect of reflections off the voids, which gives a more accurate reading.

As can be seen in Figure 5a there is a single definitive peak. The rest of the surface is not an ideal flat plane of zero values, due to the complex nature of a real seismogram. The cost function values were squared to enhance the signa- to-noise ratio. Figure 5b shows that the resultant peak location is roughly 20 m away from the location predicted by Trace. However, this location was determined using just a single seismogram. The peak value may not be perfect, but shows promise, especially if it shows that a single seismogram can be used to find the location of the event with reasonable accuracy.

The cost functions in Figure 5 show there is a large region of elevated correlations centred on node (y = 200, D = 200). Such a region can be explained as due to numerical artefacts resulting from performing the cross-correlations across the entire waveforms. Using Pythagoras it can be calculated that the maximal peak located at (y = 123 , D = 99) in Figure 5 is roughly 78 m away from the sensor.

Figure 6a shows the comparison of the data trace in red as well as the linear combination of library tensors in blue. We used the seismogram to calculate the path distance from source to sensor. Equation [7] shows the derivation of finding the distance, d, in terms of the P-wave arrival time (t_p) and velocity (v_p) and the S-wave arrival time (t_s) and velocity (vs) and an initial time (t_0). Picking the P- and S-wave arrival points at 330 and 430, respectively, and the standard velocities of 6 km/s for P-waves and 3.73 km/s for S-waves, the calculated distance, using Equation [7], was found to be 80 m.

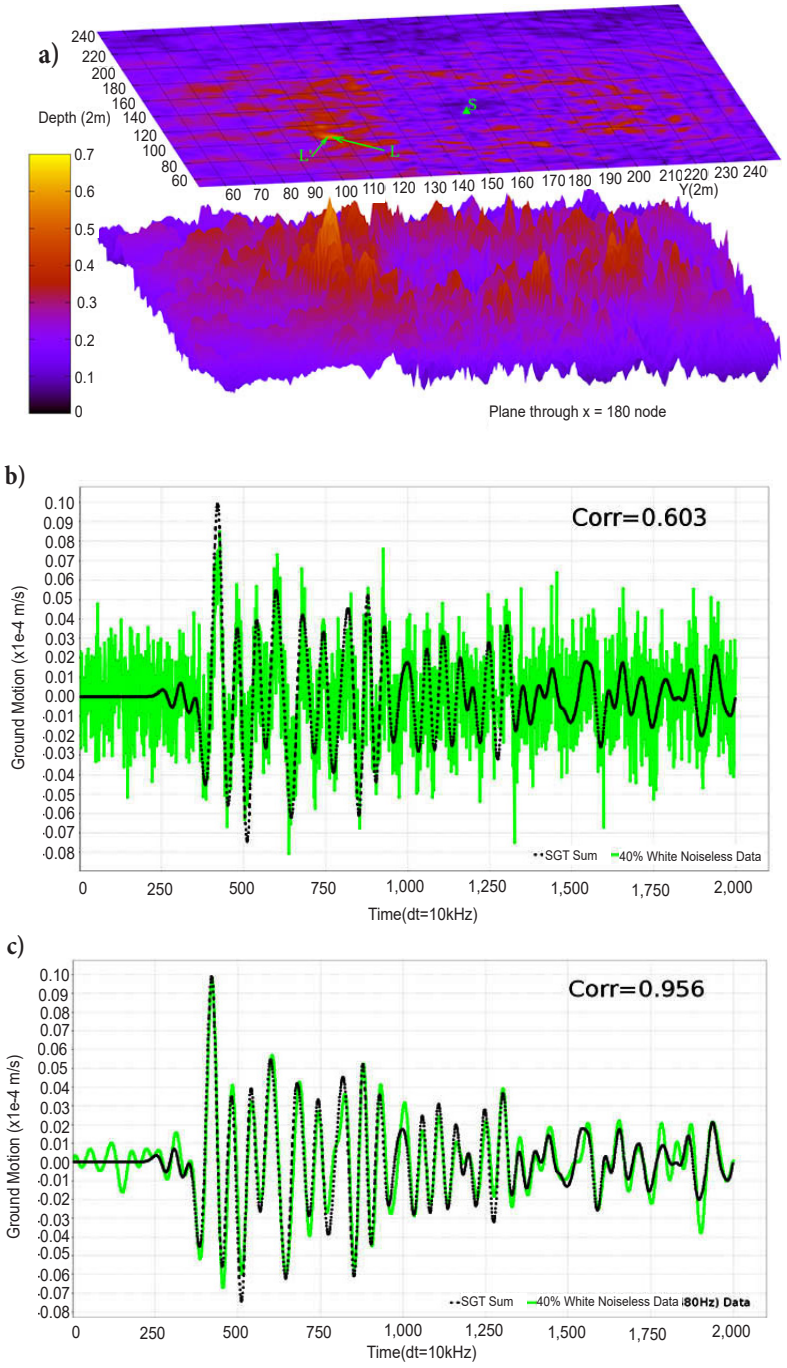

Figure 4—Results of correlating a 250Hz data trace contaminated with 40% white noise against a library of noiseless strain Green's tensors. a)Objective function represents x-plane through true source location (x=180) with true source, L, sensor, S, and calculated maximal location at L'. Maximal location bright spot at node (y=105, Depth=105) matches real source at node (y=105, Depth=105). Maximum correlation reaches just over 0.6 due to the high degree of noise present in the data trace. b) Summed synthetic strain Green's tensors waveform (black) vs 250Hz data trace contaminated with 40% white noise (green), showing correlation of just over 0.6. Observe most energetic sections of waves match between samples 400 to 2000. Calculated source parameters are very similar to the true source parameters. c) White noise data trace from b) band-pass filtered (20-480HZ) (green) and correlated against noiseless SGT library (black). Calculated parameters for band-pass filtered trace gives a correlation of 0.956. Noise tests show that synthetic complex waveforms that simulate real seismograms can also be used to produce definitive results

$$t_p = t_0 + d/v_p$$
$$t_s = t_0 + d/v_s$$
$$t_s - t_p = d\left(1/v_s - 1/v_p\right) \quad [7]$$
$$d = \left(t_s - t_p\right)/\left(1/v_s - 1/v_p\right)$$

This value compares very well to the distance calculated from the cost functions.

More importantly this establishes a region of interest outlined by a border of radius 80 m. Using this value, it can be seen that the region of elevated correlations in the cost functions falls outside this radius, and is therefore not physically significant.

We use the DE optimization technique to reduce the processing time.

DE works by initially comparing two waveforms created using diffferent sets of values. In our work we have ten independent parameters. The three location values, the frequency, and the six

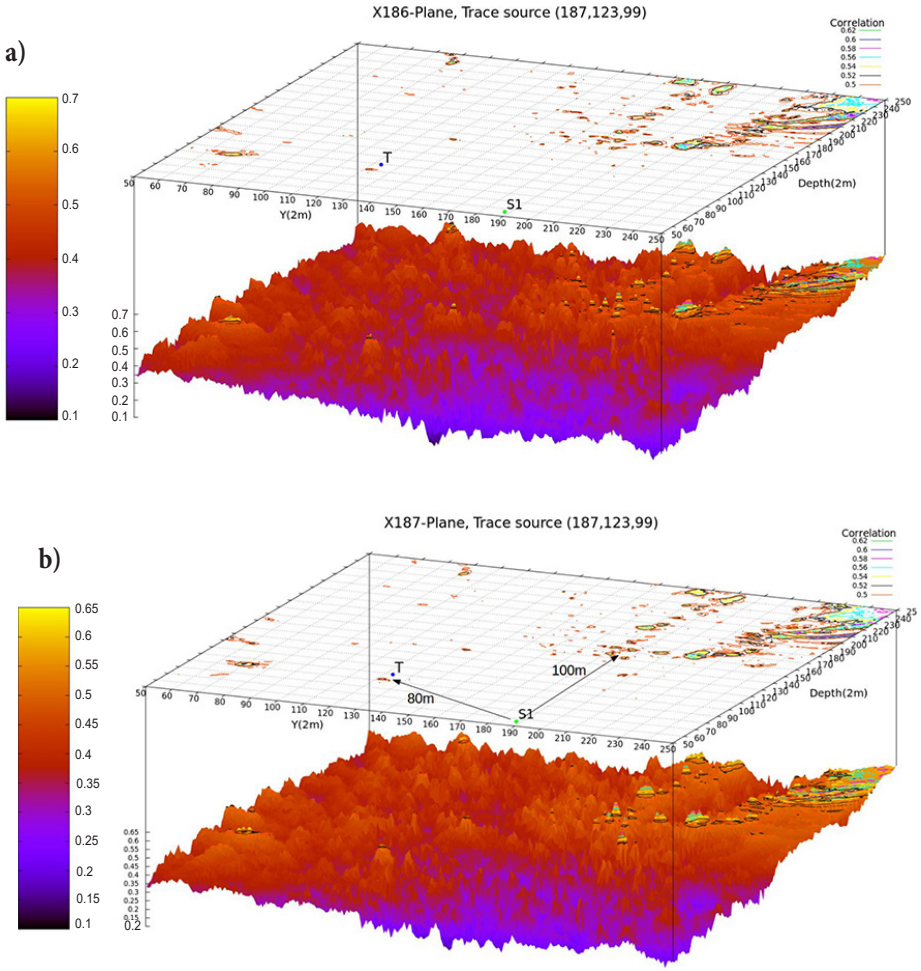

Figure 5—Cost functions for a real event (a) through maximal x=186 node plane, (b) through maximal x=187 node plane. 'T' and 'S1' labels represent Trace calculated position and sensor site, respectively

moment tensor components suffice to fully describe an event. DE creates a candidate solution using trial values for each parameter. Each parameter can be stipulated to exist within a certain range of values; this helps to optimize the processing time for the run, but also allows the algorithm to scan through a source space of potential values. DE compares a new candidate solution to the previous solution. If the new solution is an improvement in terms of being optimally maximal, then the ten values of the parameters for that solution are kept, and the other solution's parameters are disregarded. DE will take values of parameters that yield a better solution from both and combine, or mutate, them into a new solution that uses information from the previous generation.

An example of the results of DE is shown in Figure 7. The blue trace is the summed convolved SGT waveform, and the red is the event trace. Each run produced a maximal correlation of approximately 0.65. This is a significantly high value, considering the complex nature of the two waveforms. The maximal frequency of the event ranged from 355 to 480 Hz, which we averaged through oter numerous runs to 400 Hz. The maximal location in three dimensions was within a very tight locale, centred on node (x = 185, y = 123, D = 92).

Clearly the DE run circled around a maximal global location.

There is only a few metres difference between the DE maximal location and that achieved by the brute force method that created the cost functions in Figure 6. This reinforces the affirmation that our technique, in conjunction with DE, can be used as a very effective and accurate method to determine the source parameters of a microseismic event.

Conclusion

We have shown that cross-correlation of unaltered, full, complex seismograms with the strain Green's tensor library constitutes a powerful tool, as with just a single uniaxial sensor the correct location of a microseismic event is retrieved with functionally perfect correlations. The method we propose is robust as it has been shown numerically that variations in the model that are realistically non-ideal, such as unknown regions of background velocities by up to ±20% and shifts in the mine plans in relation to the sensor sites by a few metres do not drastically affect the resolution of the source location or mechanism. We have also shown that a data trace contaminated by noise can still be used to identify the source parameters. Although a highly complex waveform usually makes processing difficult, for this method it is useful as it adds to the uniqueness of the true source location. Differential evolution is a promising tool in solving the problem, as the moment tensor components of the source, the source location, and frequency can be approximated relatively well in a timeous manner. If the location of an event can be retrieved using just a single trace. This will prove to be a very powerful advancement in microseismic location estimation.

a)

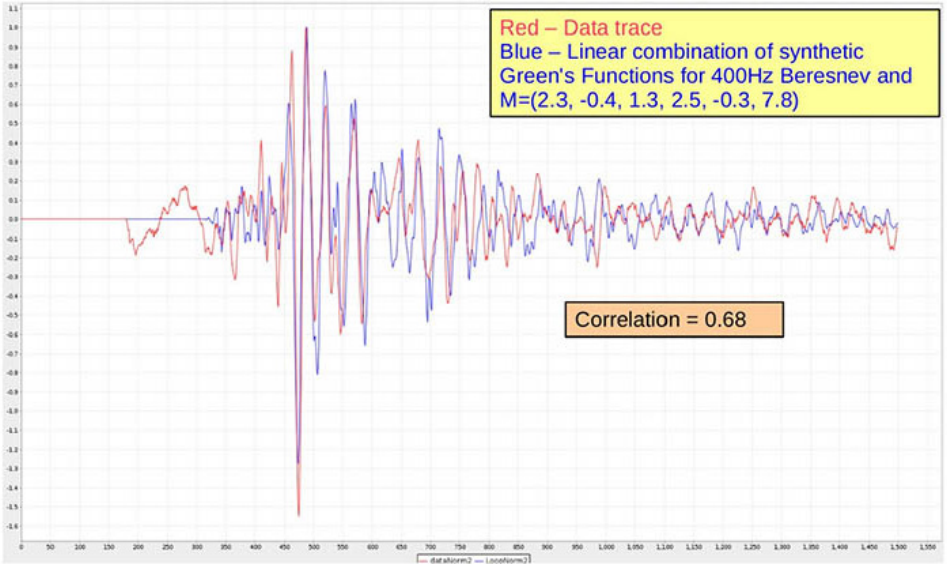

b)

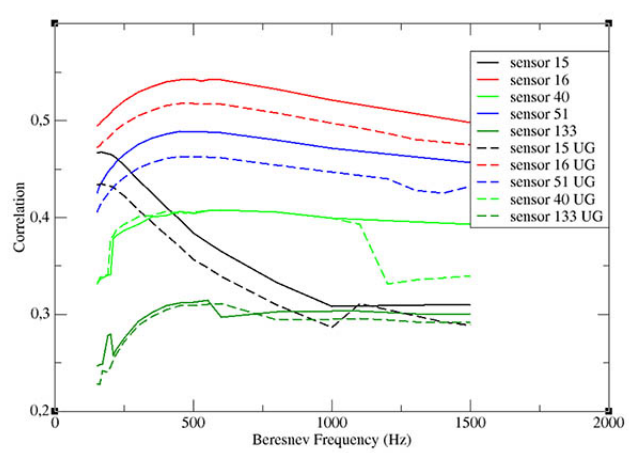

Figure 6— a) Comparison of data trace (red) versus linear combination of strain Greens Tensors (blue). b) Maximal correlation variation with frequency per sensor for single event, showing maximal correlations around 390 - 450 Hz. 'UG' means signls had leading noise before P-wave arrival zeroed out

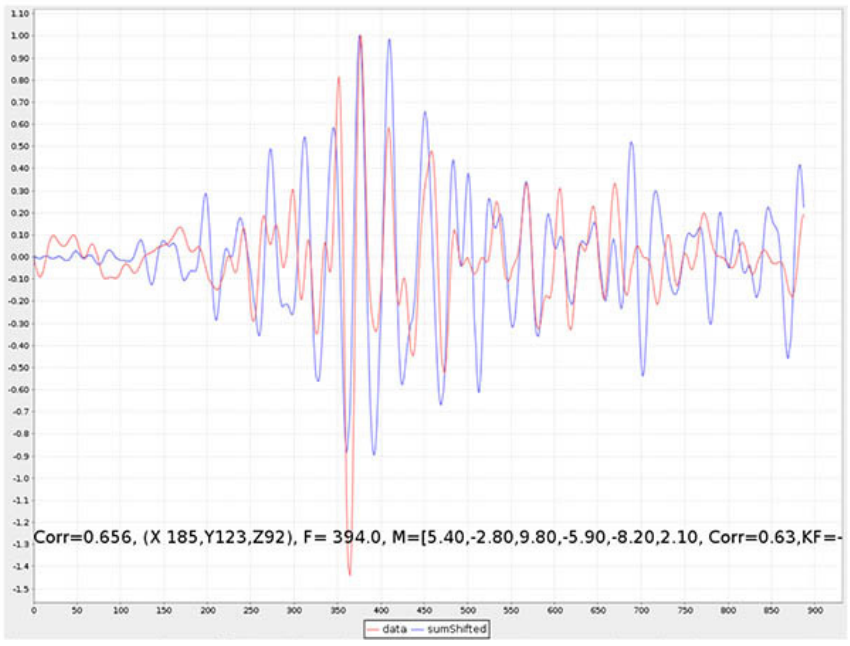

Figure 7—Comparison of full 10-dimensional traces for 16 July 2015 microseismic event recorded by sensor

References

Aki, K. and Richards, P.G. 2002. Quantitative Seismology. 2nd edn. University Science Books, Herndon, VA

Arnold, M.E. 1977. Beam forming with vibrator arrays. Geophysics, vol. 42. pp. 1321–1338.

Asch, G., Wylegalla, M., Hellweg, M., Seigi, D., and Rademaher, H. 1996. Observations of rapid-fire event tremor at Lascar volcano, Chile. *Annals of Geophysics*, vol. 39, pp. 273–282.

Gajewski, D. and Tessmer, E. 2005. Reverse modelling for seismic event characterization. *Geophysical Journal International*, vol. 163, pp. 276–284.

Geiger, L. 1912. Probability method for the determination of earthquake epicenters from the arrival time only. *Bulletin of St. Louis University.*

Gharti, H.N., Oye, V., Roth, M., and Kuhn, D. 2010, Automated microearthquake location using envelope stacking and robust global optimization. *Geophysics*, vol. 75, no. 4, pp. MA27–MA46.

Gharti, H.N., Oye, V., Kuhn, D., and Zhao, P. 2011, Simultaneous microearthquake location and moment-tensor estimation using time-reversal imaging. T *SEG Technical Program Expanded Abstracts,* vol. 30, no. 1, pp. 1632–1637. doi:10.1190/1.3627516

Iyer, H,M. and Hirahara, K. 1993. Seismic Tomography: Theory and Practice. Chapman and Hall.

Kao, H. and Shan, S.J. 2004. The source-scanning algorithm: Mapping the distribution of seismic sources in time and space. *Geophysical Journal International*, vol. 157, pp. 589–594.

Kawakatsu, H. and Montagner, J-P. 2008. Time-reversal seismic-source imaging and moment-tensor inversion. *Geophysical Journal International*, vol. 175, pp. 686–688.

Larsen, S. and Schultz, C.A. 1995a. ELAS3D: 2D/3D elastic finite difference wave propagation code. *Technical Report* no. UCRL-MA-121792. U.S. Department of Energy, Office of Scientific and Technical Information.

Larsen, S and Schultz, C.A. 1995b. ELAS3D: 2D/3D elastic finite difference wave propagation code. *Technical Repor*t no. UCRL-MA-121792. U.S. Department of Energy, Office of Scientific and Technical Information.

Lynch, R.A. and Lotter, E. 2007. Estimation of cave geometry using a constrained velocity model inversion with passive seismic data. *Journal of the Southern African Institute of Mining and Metallurgy*, vol. 107, no. 12, pp. 791–796. http://saimm.s1029.sureserver.com/Journal/v107n12p791.pdf

Mendecki, A.J. 1997. Seismic Monitoring in Mines. Chapman and Hall.

Mendecki, A.J. and Young, R.P. 1993. Real time quantitative seismology in mines. *Proceedings of the 3rd International Symposium on Rockbursts and Seismicity in Mines*, Kingston, ON. Routledge. pp. 287–295.

Ringdal, F. and Kværna, T. 1989. A multi-channel processing approach to real time network detection, phase association, and threshold monitoring. *Bulletin of the Seismological Society of America*, vol. 79, no. 1, pp. 927–1940.

Sewjee, R., Lynch, R.A., and du Toit, C. 2008. Locating seismic events in mines containing strongly heterogeneous media. *Proceedings of the Fifth International Conference and Exhibition on Mass Mining*, Luleå, Sweden. Schunnesson, H. and Nordlund, E. (eds). Luleå University of Technology.

Siwei, L. and Fomel, S. 2013. Kirchhoff migration using eikonal-based computation of traveltime source-derivatives. *Geophysics,* vol. 78, no. 4, pp. S211–S219.

Thurber, C.H. 1986. Analysis methods for kinematic data from local earthquakes. *Reviews of Geophysics*, vol. 24, pp. 793–805.

Waldhauser, F. and Ellsworth, W.L. 2000. A double-difference earthquake location algorithm: Method and application to the Northern Hayward fault, California. *Bulletin of the Seismological Society of America*, vol. 90, pp. 1353–1368.

Waldhauser, F. and Schaff, D.P. 2008. Large-scale relocation of two decades of Northern California seismicity using cross-correlation and double-difference methods. *Journal of Geophysical Research*, vol 113, B08311. ◆